Surface & Coatings Technology xxx (2016) xxx–xxx

Contents lists available at ScienceDirect

Surface & Coatings Technology

journal homepage: www.elsevier.com/locate/surfcoat

Influence of microstructures on mechanical properties and tribology behaviors of TiN/$Ti_XAl_{1-X}N$ multilayer coatings

Jingxian Wang [a,b], Mohammad Arab Pour Yazdi [c], Fernando Lomello [d], Alain Billard [c], András Kovács [e], Frederic Schuster [f], Claude Guet [a,b], Timothy J. White [a,b], Frederic Sanchette [g], ZhiLi Dong [a,*]

[a] School of Materials Science and Engineering, Nanyang Technological University,Singapore 639798, Singapore
[b] Energy Research Institute at NTU, Interdiciplinary Graduate School, Nanyang Technological University, Singapore 637141, Singapore
[c] FEMTO-ST UMR 6174, CNRS, Univ. Bourgogne Franche-comté, UTBM, F-90010 Belfort, France
[d] Den–Service d'Etudes Analytiques et de Réactivité des Surfaces (SEARS), CEA, Université Paris-Saclay, 91191 Gif sur Yvette, France
[e] Ernst Ruska-Centre for Microscopy and Spectroscopy with Electrons, Peter Grünberg Institute, Forschungszentrum Jülich, 52425, Germany
[f] CEA Cross-Cutting program on Advanced Materials Saclay, 91191 Gif-sur-Yvette, France
[g] LRC CEA-ICD-LASMIS-UTT, Antenne de Nogent-52, 52800 Nogent, France

ARTICLE INFO

Article history:
Received 3 August 2016
Revised 10 November 2016
Accepted in revised form 28 November 2016
Available online xxxx

Keywords:
Cathodic arc deposition
Nano-multilayers
Transmission electron microscope
Nanoindentation
Tribology

ABSTRACT

There are demands to form nanolayered coating consisting of different materials in order to enhance the coating mechanical properties. However, poor structure control may lead to the formation of second phase and various defects. In this work, we endeavored to use cathodic arc deposition (CAD) method to fabricate TiN/$Ti_XAl_{1-X}N$ nanolayered coatings with periods (Λ) ranging from 8 to 45 nm, which has great influences on coating microstructures and properties. X-ray diffraction (XRD), electron microscopy, nanoindentation and tribometry were employed to correlate coating microstructure and Λ with mechanical properties and wear resistance. The nanolayered coatings consisted of columnar grains with [111] texture, where individual grains contained low-angle grain boundaries without voids and amorphous phases. As Λ decreased, superlattices were generated, and reducing Λ from 45 nm to 13 nm yielded coatings with superior mechanical properties. The hardness peaked at 38.9 ± 3.6 GPa with a Young's modulus at 502.5 ± 40.4 GPa at 13 nm, however, when the Λ decreased to 8 nm the hardness and the Young's modulus deteriorated. It was concluded that wear resistance improved as the Λ decreased due to the greater interface population that impedes crack propagation.

1. Introduction

Titanium nitride (TiN) thin films produced by physical vapor deposition (PVD) are hard and wear resistant ceramics applied as protective industrial coatings, especially to improve steel tool machining efficiency and tool life time [1,2]. Compared to TiN that has limited oxidation resistance, (Ti, Al)N presents as a more promising material for high speed machining because Al diffuses to form protective Al_2O_3 surface layers, and thus presents superior oxidation resistance and high hardness in extreme environments [3,4]. Multilayered thin films consisting of two components with unique mechanical and chemical properties, when arranged as nanoscale superlattices, show hardnesses beyond rule-of-mixtures values [5,6], ascribed to the inhibition of dislocation motion through interfaces of different shear moduli [7–12] and the bilayer period (Λ) is critical to superlattice hardening.

In 1998, Hsieh et al. [13] for the first time deposited TiN/TiAlN multilayered coatings using unbalanced magnetron sputtering and revealed multilayered TiN/TiAlN coatings with a lower wear rate than single-layered TiAlN. This improvement, as reported by Anderson et al. [14], is ascribed to the wear mechanism change as adhesive wear being significantly reduced in multilayered coatings. In 2003, Weber et al. [15] deposited TiAlN/TiN multilayered coatings by cathodic arc evaporation and studied the influence of bias voltage (from −30 V to −125 V) on coated cutting tool lifetime in drilling. Cathodic arc evaporation employs a higher energy input than sputtering process and generates arc moving over target surface to evaporate metal in small areas called cathode spots. The highly ionized metal vapor allows to form high density layers. Arc deposited TiN/TiAlN multilayered coatings adopting various architectures have been investigated extensively in order to enhance hardness, biocompatibility, wear and corrosion resistance [16–18], but many of these researchers are focused on bilayer period of higher than 50 nm. The bilayer period was found to be one of the most important parameters for coating properties, and the highest hardness and wear resistance generally occur in a narrow range of 4–20 nm [19–23]. Moreover, a low thermal conductivity is also required for barrier coatings and it decreases with decreasing bilayer period in arc deposited TiN/TiAlN coatings as reported by Samani et al. [24]. The

* Corresponding author.
E-mail address: zldong@ntu.edu.sg (Z. Dong).

http://dx.doi.org/10.1016/j.surfcoat.2016.11.101
0257-8972/

lowest value of thermal conductivity was obtained with the period of 12 nm, related to microstructure features including grain size and misfit dislocation.

In the present work, TiN/$Ti_XAl_{1-X}N$ multilayered coatings deposited by cathodic arc deposition are investigated with period (Λ) ranging from 8 to 45 nm. The aim of the present letter is from a microscopic point of view to assess how the structure of varied periods (Λ) contributes to the enhancement on coating mechanical properties and tribology performances. To increase the adhesion of coatings, buffer layers consisting of Ti and TiN were deposited first and then multilayers with controllable Λ by the substrate holder rotation speed. To reveal the relationship between microstructure and properties, X-ray diffraction (XRD) and transmission electron microscopy (TEM) were applied to study cross-sectional structures, and nano-indentation measured the hardness and Young's modulus, while wear resistance was examined by tribology testing.

2. Experimental methods

The coatings were deposited by using a PLANAR system (PLATIT) equipped with 2 arc powered sources and rotating substrate holders. Coatings were fabricated using pure titanium (Ti, purity 99.99%) and aluminum-titanium alloy (Al/Ti = 60/40 at.%) sources. AISI M2 HSS substrates were polished to a mirror finish and cleaned with soap and degreased with alcohol before mounting on a substrate holder. Argon etching was performed for 2 min at 0.3 Pa (bias ≈ −800 V) followed by Ti etching (I_{Ti} = 100 A) for 10 min at 1 Pa (bias ≈ −700 V). First a Ti and a TiN buffer layer were deposited for 25 min (I_{Ti} = 100 A; bias ≈ −100 V; N_2 flow = 110 sccm) to increase coating adhesion. Then the multilayer coatings were deposited at ~400 °C for 50 min. The substrate holder rotation rate was varied from 1 to 7 revolution per minute (r.p.m). During deposition, the substrate bias voltage was −100 V and the arc current applied on both targets was 100 A. Deposition was conducted under pure N_2 at a flow of 110 sccm and a chamber pressure of ~2 Pa. The final coating thickness was 4.1 μm, inclusive of a Ti layer and a TiN buffer layer that are around 0.6 μm and 0.4 μm respectively.

The fracture cross-section and surface morphology were observed by field emission scanning electron microscopy (FE-SEM JEOL 7800F) in the secondary electron imaging (SEI) mode. The XRD patterns were recorded by using a Brucker D8 Focus instrument (Bragg–Brentano θ–2θ geometry; CoKα1 radiation, λ = 1.788970 Å). Conventional TEM and scanning transmission electron microscopy (STEM) (JEOL JEM-2100F) were employed to observe the nanostructure at an accelerating voltage of 200 kV. High-resolution images were obtained with a TEM FEI Titan at 300 kV. The coating compositions were determined by energy dispersive X-ray spectroscopy (EDX) in STEM mode. Samples were prepared for TEM by depositing the coatings on copper foils, sticking the samples face to face, cross sectioning and mechanically polishing to 30 μm and finally argon ion milling (Precision Ion Polishing System, Gatan) to the appearance of an electron transparent edge.

Hardness (H) and effective Young's modulus (E^*) were measured by means of a nanoindentation tester (NHT CSM Instrument) equipped with a Berkovich diamond tip. The maximum load was 20 mN, and the loading and unloading rates were 10 mN/min. Final results were averaged from 10 indentations with imposed penetration depths < 10% of the coating thickness in order to exclude substrate influence [25]. The Oliver and Pharr method was employed to determine both values [26]. The tribological performance was evaluated by conducting ball-on-disc tests (CSM tribometer) with 6 mm-diameter WC/Co balls as the counter material. A constant load of 10 N was applied on the ball with a wear track radius of 9 mm, a sliding distance of 565 m (10,000 laps) and a sliding velocity of 100 mm/s. The tests were performed in air at room temperature (20–23 °C) at a relative humidity of 50%–55%. The wear scar was examined by a white-light profilometer (ALTISURF500) in 2D profile mode to a height resolution of 10 nm with a scanning speed fixed at 15 μm/s.

3. Results and discussion

3.1. Coating processing with controlled Λ

The period (Λ) of multilayered coatings could vary discretely by controlling the substrate rotation speed. The cross-section of the 1 r.p.m. sample is presented in Fig. 1(a). The Λ thickness were determined and confirmed using a combination of TEM observations and XRD patterns (see Section 3.2.1). The multilayers appear with alternating contrast (TiN is in dark and $Ti_XAl_{1-X}N$ is in bright), with Λ decreasing inversely with sample holder rotation speed (Fig. 1(b)–(c)). The fitting plot showing Λ^{-1} proportional to rotation speed (Fig. 1(d)) is consistent with C. Ducros et al. [27]. Thus Λ (8–45 nm) and rotation were correlated with current deposition parameters.

3.2. Structural and composition analysis

3.2.1. Structure analysis-diffraction patterns

XRD patterns confirm the fcc NaCl-rocksalt structure (Fig. 2), but with an intense (111) reflection and an absence of (002) comparing with the simulated TiN powder pattern (ICSD-644780 [28]) (Fig. 2(c)), indicating a (111) coating texture. The film deposited at 1 r.p.m. (Λ = 45 nm) shows two distinct (111) peaks that can be assigned to TiN (a = 4.27(0) Å) and $Ti_XAl_{1-X}N$ phases (a = 4.19(0) Å) respectively after fitting. With increasing rotation speed and decreasing Λ, the two (111) peaks progressively merge to a primary centered peak bracketed by satellite peak pairs, especially above 4 r.p.m. (Λ ≤ 14 nm), that is characteristic of a superlattice structure. Satellites were prominent when Λ ≤ 14 nm. The lattice parameters of the superlattice are intermediate to TiN and $Ti_XAl_{1-X}N$. For clarity, XRD patterns accumulated with a slower scan speed of 0.004° 2θ s^{-1} from 2θ = 40° to 46° confirm the satellites are further from the central peak as Λ decreases (Fig. 2(b)). The Λ can be calculated from the separation of the main peaks and satellites according to the relationship: $\sin\theta_{\pm} = \sin\theta_B \pm m_{th}\lambda/(2\Lambda)$, where $\theta_{\pm}$ is

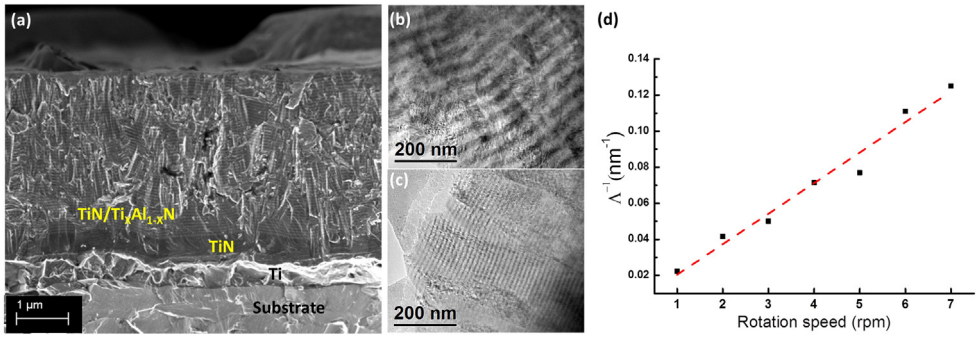

Fig. 1. SEM fracture of TiN/$Ti_XAl_{1-X}N$ coatings when rotation speed = 1 r.p.m (a); TEM cross sections when rotation = (b) 1 r.p.m., and (c) 4 r.p.m; (d) the graph of Λ^{-1} vs rotation speed.